Effects of range size on species–area relationships

Andrew P. Allen* and Ethan P. White

*Department of Biology, University of New Mexico, 167 Castetter Hall,
Albuquerque NM 87131-1091, USA*

ABSTRACT

It has been known for some time that the slope of the species–area relationship increases asymptotically at broad spatial scales when richness is plotted against area on logarithmic axes. At continental to global scales, species–area relationships are determined to a large extent by the abundance and size distribution of species ranges. Here we present an analytical model that explicitly quantifies the effects of range size on species–area relationships. The model shows how range size and plot area interact to control the form of species–area relationships at broad spatial scales. It also demonstrates how changes in spatial scale affect biodiversity patterns by changing the relative influence of range size and range abundance on species richness. Our model provides an explanation for the broad-scale upturn of the species–area relationship, but more work is needed to incorporate the effects of range size, habitat heterogeneity, individual sampling and other variables into a unified framework that can account for species–area relationships at all scales.

Keywords: biodiversity, macroecology, power law, range size, spatial scale, species–area relationship, species richness.

INTRODUCTION

The increase in the number of species, S, with plot area, A_P, is one of the oldest documented patterns in ecology (Rosenzweig, 1995). Continental species–area relationships consist of three major sub-patterns (Fig. 1) (Williams, 1943; Preston, 1960; Rosenzweig, 1995). At very small spatial scales, richness increases with area primarily as a consequence of sampling greater numbers of individuals. This phase typically appears concave down on a log–log plot, but its exact form depends on the frequency distribution of species abundance (Arrhenius, 1921; Coleman, 1981; Hubbell, 2001). At intermediate scales, the increase in richness often takes the form of a power law ($S \propto A_P^Z$), with the exponent z usually falling between 0.1 and 0.25 (Arrhenius, 1921; Preston, 1962; Rosenzweig, 1995; Kunin, 1998; Harte *et al.*, 1999; Hubbell, 2001). This power function may hold over a broad range of scales. Explanations invoked to explain this pattern include habitat heterogeneity (Rosenzweig, 1995), self-similar species distributions (Harte *et al.*, 1999) and dispersal limitation (Hubbell, 2001). Finally, as the plot area expands to encompass entire continents and the globe, the power-law exponent is no longer constant, but instead increases

---

* Author to whom all correspondence should be addressed. e-mail: drewa@unm.edu
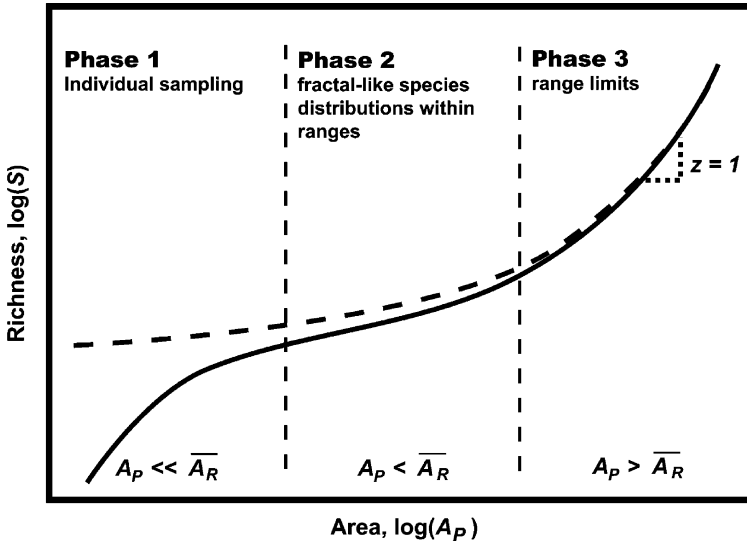
Fig. 1. Three phases of the species–area relationship on a log–log plot. Two lines are presented, an idealized empirical species–area relationship (solid line) and an upper bound on richness computed based on the abundance and size distribution of species ranges (dotted line). Empirical species–area relationships always have fewer species than the upper bound because no species is present at all points within its range. In Phase 1 of the empirical species–area relationship, there is a rapid increase in species with area as a consequence of individual sampling. In Phase 2, processes generating fractal-like distributions of species operate to produce power laws with slopes (z exponents) that are relatively constant on a log–log scale and < 1. At some point during Phase 3, plot area exceeds average range size for the first time ($A_P > \overline{A_R}$), the slope increases asymptotically to $z = 1$, and the empirical species–area relationship and the upper bound approach equality.

asymptotically towards $z = 1$ (Williams, 1943; Preston, 1960; Brown, 1995; Rosenzweig, 1995; Hubbell, 2001). It has been proposed that this increase is caused by the inclusion of multiple biological provinces with distinct evolutionary histories (Williams, 1943; Rosenzweig, 1995).

Here we present a simple mathematical model to account for the increasing slope of the species–area relationship at broad spatial scales that is based entirely on the interaction between the geometry of species ranges and sampling plots. Similar ideas have already been presented conceptually and via simulation (e.g. Leitner and Rosenzweig, 1997; Maurer, 1999; Hubbell, 2001). Most recently, McGill and Collins (2003) have shown that simulations of randomly distributed species ranges can fit the upper scales of the species–area relationship for birds of North America. This paper will derive such a model analytically using two simplifying assumptions: (1) ranges are randomly distributed in space irrespective of size and geographic location and (2) ranges are circular in shape.

MODEL ASSUMPTIONS AND PARAMETERS

Assumption 1: Ranges are randomly distributed in space

Biologically, this assumption implies that species are independently distributed with respect to environmental gradients (Gleason, 1926), that there are no geographic gradients in

species richness or range size and that there are no 'mid-domain effects' *sensu* Colwell and Hurtt (1994), constraining the placement of ranges of different size within a region. Mathematically, this assumption implies that range centroids follow a spatial Poisson process (Diggle, 1983). We characterize the 'intensity' of this process in the model using the parameter S_D, which is the average number of range centroids per unit area.

Assumption 2: Ranges are circular

This assumption is always violated in nature, but can be justified if species ranges are relatively compact in shape and show no tendency to be elongated in a particular direction. The effective radius of the range, R_i, for species i can be approximated by the radius of a circle whose area is equal to that of the range A_R ($R_i = \sqrt{A_R/\pi}$). This approximation is reasonable provided that the range is close to circular and has no holes inside of it. Otherwise, R_i should be calculated as the square root of the mean squared-distance between the range edge and range centroid.

Together, Assumptions 1 and 2 imply that the frequency distribution of range sizes can be characterized entirely by a geographically invariant probability density function $f(R)$, where $f(R)\mathrm{d}r$ is the proportion of species ranges in the size interval centred on radius R of width $\mathrm{d}r$. The function $f(R)$ can be a theoretical distribution or it can be generated empirically based on the observed values of R_i for the species assemblage. The only restrictions on $f(R)$ are that its mean, $\bar{R}$, and variance, σ^2, exist, and that it be defined only for $R \geq 0$. These restrictions imply that the integral of $f(R)$ from 0 to infinity is $\int_0^\infty f(R)\mathrm{d}r = 1$, that the average range radius is $\bar{R} = \int_0^\infty f(R)R\mathrm{d}r$, and that the average range area is $\bar{A}_R = \pi \int_0^\infty f(R)R^2\mathrm{d}r$.

Assuming that the range radii for all species are equal to the same constant value of R_i, the average number of species ranges that will overlap a point is

$$S = S_D \pi R_i^2 = S_D A_R \tag{1}$$

Equation (1) holds because all ranges whose centroids lie within radius R_i and area A_R ($= \pi R_i^2$) of a point will overlap that point (Fig. 2a), and because the expected number of centroids in an area of size A_R is $S_D A_R$. This expectation is a well-known property of spatial Poisson processes (Diggle, 1983). Using similar reasoning, equation (1) can be extended to the case where richness is estimated not at a point, but in a circular plot of radius P (Fig. 2b):

$$S = S_D \pi (R_i + P)^2 \tag{2}$$

As expressed in equation (2), richness is a function of the density of range centroids, the radius of the plot and the constant range radius R_i.

We can introduce variation in range size among species by calculating S as

$$S = S_D \pi \int_0^\infty f(R)(R + P)^2 \, \mathrm{d}r = S_D \bar{A}_R + S_D A_P + 2 S_D \bar{R}\sqrt{\pi A_P} \tag{3}$$

Note that two measures of range size enter into the richness calculation, average range area and average range radius. Note also that $\sigma^2 = \overline{R^2} - \bar{R}^2$, which implies that $\bar{A}_R = \pi(\sigma^2 + \bar{R}^2)$. Substituting this alternative expression for average range area into the right-hand side of equation (3) demonstrates that explicit integration of the function is unnecessary if the mean and variance of $f(R)$ are already known.
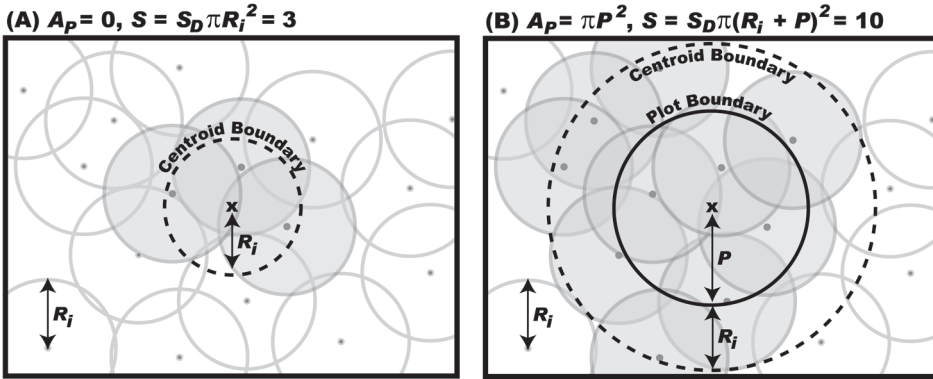
Fig. 2. Graphical depiction of how richness is calculated for (A) a point x and for (B) a plot of radius P centred on x. Grey circles represent Poisson-distributed species ranges, which all have the same radius R_i in this simple example. In (A), all ranges whose centroids (grey dots) lie within the boundary of radius R_i and area A_R $(= \pi R_i^2)$ of the point x (black, dashed-line circle) overlap x and are darkened. In (B), all ranges whose centroids lie within a boundary of radius $R_i + P$ and area $\pi(R_i + P)^2$ (black, dashed-line circle) overlap the plot (black, solid-line circle) and are darkened.

Taking the derivative of S with respect to plot area in equation (3) yields

$$dS/dA_P = S_D(1 + \overline{R}\sqrt{\pi/A_P}) \qquad (4)$$

Equation (4) reveals that, for large A_P, the slope of the relationship between richness and plot area approaches S_D; this is the slope of the upper 'limiting tangent' of Preston (1960). On a log–log scale, the slope of the relationship between S and A_P is $d\log S/d\log A_P = (A_P/S) \times (dS/dA_P)$, which is also the exponent z of the species–area relationship. Substituting equations (3) and (4) into this equation yields

$$z = (A_P/S)(dS/dA_P) = (A_P + \overline{R}\sqrt{\pi A_P})/(\overline{A_R} + A_P + 2\overline{R}\sqrt{\pi A_P}) \qquad (5)$$

Equation (5) reveals that z is always < 1, but approaches 1 asymptotically as the plot area expands to encompass an area much greater than that of species ranges. In the special case where plot area and average range area are equal in magnitude ($\overline{A_R} = A_P$), equation (5) predicts that $z = \frac{1}{2}$ for all $f(R)$.

We performed a series of computer simulation trials to demonstrate the analytical derivation of the model. Each simulation trial involved four steps: (i) randomly placing 10,000 range centroids on a 100×100 unit lattice to simulate a Poisson spatial process of intensity $S_D = 1$ species·unit^{-2} [10,000 species/(100)^2 units^2 = 1 species·unit^{-2}]; (ii) randomly assigning a range size to each centroid by sampling from $f(R)$; (iii) placing concentric circular plots of increasing size, A_P, in the centre of the lattice; and (iv) counting the number of species ranges overlapping the plots to calculate richness.

RESULTS AND DISCUSSION

Numerical simulations were performed for three different range size distributions $f(R)$: constant, log-normal and exponential (Fig. 3, lower panels). These distributions were chosen to have identical values for mean radius ($\overline{R} = 10$) but different variances ($\sigma^2 = 0$, 10

(A) constant distribution
$\bar{R} = 10$, $\sigma^2 = 0$

(B) lognormal distribution
$\bar{R} = 10$, $\sigma^2 = 10$

(C) exponential distribution
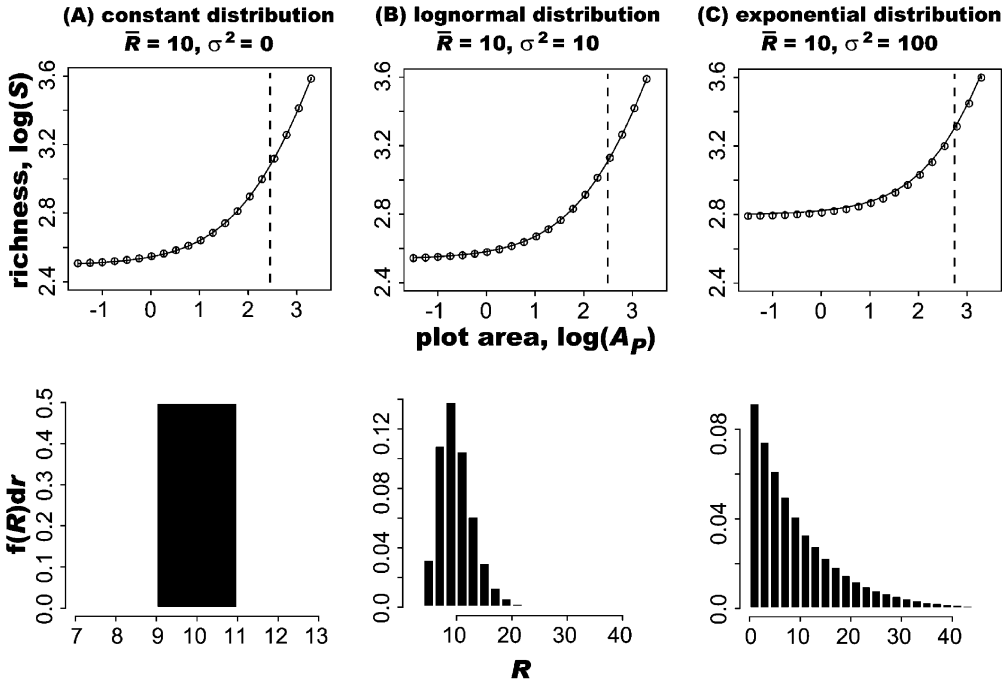$\bar{R} = 10$, $\sigma^2 = 100$

Fig. 3. Comparison of species–area relationships predicted analytically by equation (3) (lines in upper panels) to those generated numerically based on 50 simulation runs (averages of $\log_{10}$(richness) represented by points). Simulations were performed for three range size distributions (constant, log-normal and exponential; histograms in lower panels). We used the simulation data to compute and plot 95% confidence intervals for $\log_{10}$(richness), but they are too small to be clearly seen in the upper panels. Analytical predictions were within the confidence intervals in all cases. For perspective, dashed lines have been added where plot area and average range area are equal in magnitude ($\bar{A}_R = A_P$).

and 100, respectively). Three observations are worth noting in Fig. 3. First, the results of the numerical simulations (points in upper panels) are in close agreement with the predictions of equation (3) (lines in upper panels). Second, the shape of the species–area relationship changes systematically, moving from the constant distribution with 0 variance in range radius (Fig. 3a) to the log-normal and exponential distributions, which have progressively greater variances (Figs 3b and 3c). Holding $\bar{R}$, A_P and S_D constant, richness increases systematically with variance in range radius because concomitant increases in average range area (recall that $\bar{A}_R = \pi(\sigma^2 + \bar{R}^2)$) result in greater range overlap. This result is true in general because *all* $f(R)$ distributions that share the same mean and variance will have identical species–area relationships regardless of their shape (e.g. distribution skewness or kurtosis). The third observation is that when $\bar{A}_R = A_P$ (vertical lines in Fig. 3), the slopes of the species–area relationships are identical on a log–log scale; according to the model, the slope $z = \frac{1}{2}$.

It is important to note that our simple model is incomplete in that it cannot account for Phase 1 or Phase 2 of the continental species–area relationship (Fig. 1). Instead, it predicts the upper bound on richness, which is driven entirely by the abundance and size

distribution of species ranges. The model overestimates richness during Phases 1 and 2 of the species–area relationship simply because no species is present at all locations within its range.

Nevertheless, the model does provide insight into the behaviour of species–area relationships during Phase 3, as demonstrated by the recent analysis of McGill and Collins (2003). Plot area, the abundance of ranges and the sizes of ranges all enter into the richness calculation (equation 3). It is the interaction among variables that accounts for the asymptotic increase of the species–area relationship to a slope of S_D on a linear scale (equation 4), and a slope of $z = 1$ on a log–log scale (equation 5).

An important consequence of this interaction is that changes in spatial scale (A_P) will alter the relative influence of range size and range abundance (S_D) on richness. We consider two extreme cases to emphasize this point. First, if $A_P \gg A_R$, then $S \approx S_D A_P$, and geographic gradients in richness are driven almost entirely by variation in range abundance. At the opposite extreme, if $A_P = 0$ (i.e. 'point' estimates of richness are calculated as in Fig. 2a), $S = S_D \overline{A_R}$, which implies that range abundance and range size may both contribute equally to richness. This is biologically significant because there is evidence that, for many taxonomic groups, range abundance decreases, and range size increases, moving away from the equator (Stevens, 1989). Any comprehensive theory of biodiversity will need to account for geographic variation in both of these variables.

We conclude by considering methodological implications of the model. In broad-scale biodiversity studies, it is common to generate richness maps by first overlaying a grid onto geographic range distributions and then calculating the number of ranges that overlap each grid cell. Grid cell size (represented by A_P in our model) is often chosen arbitrarily. However, the selection of a particular cell size entails an implicit decision regarding the weighting given to range size and range abundance in any analyses performed using the data. Multi-scale biodiversity studies often use the same underlying range maps to generate a series of richness maps that vary in grid cell size (e.g. Rahbek and Graves, 2001). These studies often find that the environmental correlates of richness change with the size of the grid cell, perhaps reflecting differences in the environmental controls on range size versus range abundance. This example highlights the need for further work assessing the biological mechanisms underlying scale-dependent changes in biodiversity patterns.

REFERENCES

Arrhenius, O. 1921. Species and area. *J. Ecol.*, **9**: 95–99.
Brown, J.H. 1995. *Macroecology*. Chicago, IL: University of Chicago Press.
Coleman, B.D. 1981. On random placement and species–area relationship. *Math. Biosci.*, **54**: 191–215.
Colwell, R.K. and Hurtt, G.C. 1994. Nonbiological gradients in species richness and a spurious rapoport effect. *Am. Nat.*, **144**: 570–595.

Diggle, P.J. 1983. *Statistical Analysis of Spatial Point Patterns*. New York: Academic Press.

Gleason, H.A. 1926. The individualistic concept of the plant association. *Bull. Torrey Bot. Club*, **53**: 7–26.

Harte, J., Kinzig, A. and Green, J. 1999. Self-similarity in the distribution and abundance of species. *Science*, **284**: 334–336.

Hubbell, S.P. 2001. *A Unified Neutral Theory of Biodiversity and Biogeography*. Princeton, NJ: Princeton University Press.

Kunin, W.E. 1998. Extrapolating species abundance across spatial scales. *Science*, **281**: 1513–1515.

Leitner, W.A. and Rosenzweig, M.L. 1997. Nested species–area curves and stochastic sampling: a new theory. *Oikos*, **79**: 503–512.

Maurer, B.A. 1999. *Untangling Ecological Complexity: The Macroscopic Perspective*. Chicago, IL: University of Chicago Press.

McGill, B. and Collins, C. 2003. A unified theory for macroecology based on spatial patterns of abundance. *Evol. Ecol. Res.*, **5**: 469–492.

Preston, F.W. 1960. Time and space and the variation of species. *Ecology*, **41**: 611–627.

Preston, F.W. 1962. The canonical distribution of commonness and rarity. *Ecology*, **43**: 185–215.

Rahbek, C. and Graves, G.R. 2001. Multiscale assessment of patterns of avian species richness. *Proc. Natl. Acad. Sci. USA*, **98**: 4534–4539.

Rosenzweig, M.L. 1995. *Species Diversity in Space and Time*. Cambridge: Cambridge University Press.

Stevens, G.C. 1989. The latitudinal gradient in geographical range: how so many species coexist in the tropics. *Am. Nat.*, **133**: 240–256.

Williams, C.B. 1943. Area and number of species. *Nature*, **152**: 264–267.